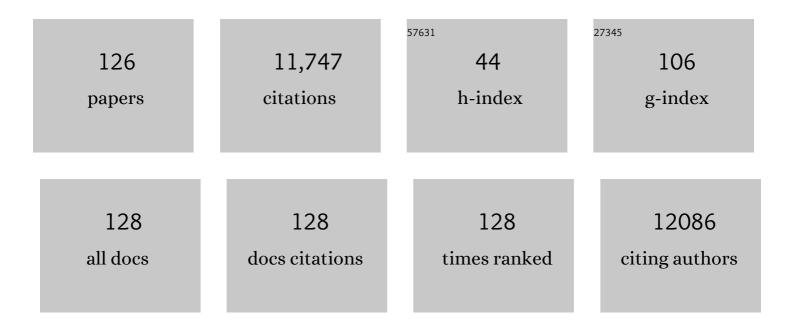
Binsheng Zhao

List of Publications by Year in descending order

Source: https://exaly.com/author-pdf/11578147/publications.pdf Version: 2024-02-01



RINSHENC 7HAO

#	Article	IF	CITATIONS
1	Effect of CT image acquisition parameters on diagnostic performance of radiomics in predicting malignancy of pulmonary nodules of different sizes. European Radiology, 2022, 32, 1517-1527.	2.3	14
2	Early Readout on Overall Survival of Patients With Melanoma Treated With Immunotherapy Using a Novel Imaging Analysis. JAMA Oncology, 2022, 8, 385.	3.4	44
3	Using virtual clinical trials to determine the accuracy of Al-based quantitative imaging biomarkers in oncology trials using standard-of-care CT. , 2022, , .		Ο
4	Association of early tumor growth rate and survival outcomes in first-line metastatic non–small cell lung cancer (mNSCLC) Journal of Clinical Oncology, 2022, 40, 9063-9063.	0.8	0
5	Comparing RECIST 1.1 and iRECIST in advanced melanoma patients treated with pembrolizumab in a phase Il clinical trial. European Radiology, 2021, 31, 1853-1862.	2.3	10
6	Identifying Robust Radiomics Features for Lung Cancer by Using In-Vivo and Phantom Lung Lesions. Tomography, 2021, 7, 55-64.	0.8	8
7	Understanding Sources of Variation to Improve the Reproducibility of Radiomics. Frontiers in Oncology, 2021, 11, 633176.	1.3	58
8	Uncontrolled Confounders May Lead to False or Overvalued Radiomics Signature: A Proof of Concept Using Survival Analysis in a Multicenter Cohort of Kidney Cancer. Frontiers in Oncology, 2021, 11, 638185.	1.3	10
9	Predicting Tyrosine Kinase Inhibitor Treatment Response in Stage IV Lung Adenocarcinoma Patients With EGFR Mutation Using Model-Based Deep Transfer Learning. Frontiers in Oncology, 2021, 11, 679764.	1.3	7
10	Distinguishing benign and malignant lesions on contrast-enhanced breast cone-beam CT with deep learning neural architecture search. European Journal of Radiology, 2021, 142, 109878.	1.2	9
11	Radiomic signatures to predict survival in patients with advanced hepatocellular carcinoma (HCC) treated with sorafenib +/- doxorubicin: Correlative science from CALCB 80802 (Alliance) Journal of Clinical Oncology, 2021, 39, 343-343.	0.8	0
12	Deep learning for the prediction of early on-treatment response in metastatic colorectal cancer from serial medical imaging. Nature Communications, 2021, 12, 6654.	5.8	29
13	819â€Radiomic markers associated with clinical benefit in advanced uveal melanoma patients with radiographic progression on tebentafusp. , 2021, 9, A857-A857.		1
14	Convolutional Neural Network Addresses the Confounding Impact of CT Reconstruction Kernels on Radiomics Studies. Tomography, 2021, 7, 877-892.	0.8	1
15	Automated Identification of Optimal Portal Venous Phase Timing with Convolutional Neural Networks. Academic Radiology, 2020, 27, e10-e18.	1.3	11
16	Radiomics machine-learning signature for diagnosis of hepatocellular carcinoma in cirrhotic patients with indeterminate liver nodules. European Radiology, 2020, 30, 558-570.	2.3	118
17	Imaging-guided precision medicine in non-resectable gastro-entero-pancreatic neuroendocrine tumors: A step-by-step approach. European Journal of Radiology, 2020, 122, 108743.	1.2	8
18	Enhanced Detection of Treatment Effects on Metastatic Colorectal Cancer with Volumetric CT Measurements for Tumor Burden Growth Rate Evaluation. Clinical Cancer Research, 2020, 26, 6464-6474.	3.2	16

#	Article	IF	CITATIONS
19	Differentiation of Focal-Type Autoimmune Pancreatitis From Pancreatic Ductal Adenocarcinoma Using Radiomics Based on Multiphasic Computed Tomography. Journal of Computer Assisted Tomography, 2020, 44, 511-518.	0.5	16
20	A quantitative imaging biomarker for predicting disease-free-survival-associated histologic subgroups in lung adenocarcinoma. European Radiology, 2020, 30, 3614-3623.	2.3	10
21	Using a single abdominal computed tomography image to differentiate five contrast-enhancement phases: A machine-learning algorithm for radiomics-based precision medicine. European Journal of Radiology, 2020, 125, 108850.	1.2	13
22	Radiomics Response Signature for Identification of Metastatic Colorectal Cancer Sensitive to Therapies Targeting EGFR Pathway. Journal of the National Cancer Institute, 2020, 112, 902-912.	3.0	93
23	Identification of Non–Small Cell Lung Cancer Sensitive to Systemic Cancer Therapies Using Radiomics. Clinical Cancer Research, 2020, 26, 2151-2162.	3.2	110
24	Multisite Technical and Clinical Performance Evaluation of Quantitative Imaging Biomarkers from 3D FDG PET Segmentations of Head and Neck Cancer Images. Tomography, 2020, 6, 65-76.	0.8	4
25	Radiomics Prediction of EGFR Status in Lung Cancer—Our Experience in Using Multiple Feature Extractors and The Cancer Imaging Archive Data. Tomography, 2020, 6, 223-230.	0.8	24
26	Toward radiomics for assessment of response to systemic therapies in lung cancer. Oncotarget, 2020, 11, 4677-4680.	0.8	1
27	Implementation Strategy of a CNN Model Affects the Performance of CT Assessment of EGFR Mutation Status in Lung Cancer Patients. IEEE Access, 2019, 7, 64583-64591.	2.6	15
28	Automatic liver segmentation by integrating fully convolutional networks into active contour models. Medical Physics, 2019, 46, 4455-4469.	1.6	46
29	Application of Radiomics in Predicting the Malignancy of Pulmonary Nodules in Different Sizes. American Journal of Roentgenology, 2019, 213, 1213-1220.	1.0	35
30	CT-Based Radiomics Model for Predicting Brain Metastasis in Category T1 Lung Adenocarcinoma. American Journal of Roentgenology, 2019, 213, 134-139.	1.0	25
31	The role of multimodal imaging in guiding resectability and cytoreduction in pancreatic neuroendocrine tumors: focus on PET and MRI. Abdominal Radiology, 2019, 44, 2474-2493.	1.0	8
32	Nonenhancing Component of Clear Cell Renal Cell Carcinoma on Computed Tomography Correlates With Tumor Necrosis and Stage and Serves as a Size-Independent Prognostic Biomarker. Journal of Computer Assisted Tomography, 2019, 43, 628-633.	0.5	5
33	Radiomics for Classifying Histological Subtypes of Lung Cancer Based on Multiphasic Contrast-Enhanced Computed Tomography. Journal of Computer Assisted Tomography, 2019, 43, 300-306.	0.5	62
34	Radiomics for Classification of Lung Cancer Histological Subtypes Based on Nonenhanced Computed Tomography. Academic Radiology, 2019, 26, 1245-1252.	1.3	48
35	Reliability of Radiomic Features Across Multiple Abdominal CT Image Acquisition Settings: A Pilot Study Using ACR CT Phantom. Tomography, 2019, 5, 226-231.	0.8	28
36	A Web-Based Response-Assessment System for Development and Validation of Imaging Biomarkers in Oncology. Tomography, 2019, 5, 220-225.	0.8	3

#	Article	IF	CITATIONS
37	Baseline and longitudinal quantification of lean muscle mass using routine CT measurements prior to resection for pancreatic adenocarcinoma Journal of Clinical Oncology, 2019, 37, 198-198.	0.8	0
38	Role of radiomics to differentiate benign from malignant pheochromocytomas and paragangliomas on contrast enhanced CT scans Journal of Clinical Oncology, 2019, 37, e14596-e14596.	0.8	4
39	Lymph node segmentation by dynamic programming and active contours. Medical Physics, 2018, 45, 2054-2062.	1.6	9
40	Visceral fat area, not body mass index, predicts postoperative 30-day morbidity in patients undergoing colon resection for cancer. International Journal of Colorectal Disease, 2018, 33, 1019-1028.	1.0	32
41	Comparison of tumor size assessments in tumor growth inhibition-overall survival models with second-line colorectal cancer data from the VELOUR study. Cancer Chemotherapy and Pharmacology, 2018, 82, 49-54.	1.1	12
42	Does breast MRI background parenchymal enhancement indicate metabolic activity? Qualitative and 3D quantitative computer imaging analysis. Journal of Magnetic Resonance Imaging, 2018, 47, 753-759.	1.9	19
43	Vol-PACT: A Foundation for the NIH Public-Private Partnership That Supports Sharing of Clinical Trial Data for the Development of Improved Imaging Biomarkers in Oncology. JCO Clinical Cancer Informatics, 2018, 2, 1-12.	1.0	14
44	CT Slice Thickness and Convolution Kernel Affect Performance of a Radiomic Model for Predicting EGFR Status in Non-Small Cell Lung Cancer: A Preliminary Study. Scientific Reports, 2018, 8, 17913.	1.6	62
45	Early response metrics for predicting trial outcomes: A report from volumetric CT for precision analysis of clinical trials (Vol-PACT) Journal of Clinical Oncology, 2018, 36, 3581-3581.	0.8	0
46	The effects of iterative reconstruction in CT on low-contrast liver lesion volumetry: a phantom study. Proceedings of SPIE, 2017, , .	0.8	1
47	Post-anoxic quantitative MRI changes may predict emergence from coma and functional outcomes at discharge. Resuscitation, 2017, 117, 87-90.	1.3	13
48	Multiâ€site quality and variability analysis of 3D FDG PET segmentations based on phantom and clinical image data. Medical Physics, 2017, 44, 479-496.	1.6	22
49	Impact of Variability in Portal Venous Phase Acquisition Timing in Tumor Density Measurement and Treatment Response Assessment: Metastatic Colorectal Cancer as a Paradigm. JCO Clinical Cancer Informatics, 2017, 1, 1-8.	1.0	17
50	Reply to A. Braillon, M. Boulin et al, and JH. Zhong et al. Journal of Clinical Oncology, 2017, 35, 258-259.	0.8	1
51	Interobserver variability in tumor contouring affects the use of radiomics to predict mutational status. Journal of Medical Imaging, 2017, 5, 1.	0.8	25
52	Pharmaco-kinetics/dynamics (PK/PD) evaluation and individual patient cross-over studies with growth trajectory assessment to adaptively develop ilorasertib Journal of Clinical Oncology, 2017, 35, 2563.	0.8	1
53	Radiomics of Lung Nodules: A Multi-Institutional Study of Robustness and Agreement of Quantitative Imaging Features. Tomography, 2016, 2, 430-437.	0.8	108
54	Quantitative 3D breast magnetic resonance imaging fibroglandular tissue analysis and correlation with qualitative assessments: a feasibility study. Quantitative Imaging in Medicine and Surgery, 2016, 6, 144-150.	1.1	9

#	Article	IF	CITATIONS
55	Assessing Agreement between Radiomic Features Computed for Multiple CT Imaging Settings. PLoS ONE, 2016, 11, e0166550.	1.1	128
56	Defining a Radiomic Response Phenotype: A Pilot Study using targeted therapy in NSCLC. Scientific Reports, 2016, 6, 33860.	1.6	189
57	Volumetry of lowâ€contrast liver lesions with CT: Investigation of estimation uncertainties in a phantom study. Medical Physics, 2016, 43, 6608-6620.	1.6	8
58	Multimodal imaging patterns predict survival in recurrent glioblastoma patients treated with bevacizumab. Neuro-Oncology, 2016, 18, 1680-1687.	0.6	94
59	Assessment of Imaging Modalities and Response Metrics in Ewing Sarcoma: Correlation With Survival. Journal of Clinical Oncology, 2016, 34, 3680-3685.	0.8	17
60	Reproducibility of radiomics for deciphering tumor phenotype with imaging. Scientific Reports, 2016, 6, 23428.	1.6	386
61	Monitoring Metastasis and Cachexia in a Patient with Breast Cancer: A Case Study. Clinical Medicine Insights: Oncology, 2016, 10, CMO.S40479.	0.6	22
62	Three-Dimensional Quantitative Validation of Breast Magnetic Resonance Imaging Background Parenchymal Enhancement Assessments. Current Problems in Diagnostic Radiology, 2016, 45, 297-303.	0.6	11
63	Algorithm Variability in the Estimation of Lung Nodule Volume From Phantom CT Scans: Results of the QIBA 3A Public Challenge. Academic Radiology, 2016, 23, 940-952.	1.3	18
64	Quantitative Imaging in Cancer Clinical Trials. Clinical Cancer Research, 2016, 22, 284-290.	3.2	106
65	A Comparison of Lung Nodule Segmentation Algorithms: Methods and Results from a Multi-institutional Study. Journal of Digital Imaging, 2016, 29, 476-487.	1.6	68
66	Semiautomated Workflow for Clinically Streamlined Glioma Parametric Response Mapping. Tomography, 2016, 2, 267-275.	0.8	8
67	A Response Assessment Platform for Development and Validation of Imaging Biomarkers in Oncology. Tomography, 2016, 2, 406-410.	0.8	19
68	Changes in liver and spleen volumes after living liver donation: A report from the adultâ€ŧoâ€adult living donor liver transplantation cohort study (A2ALL). Liver Transplantation, 2015, 21, 151-161.	1.3	23
69	Semiautomatic segmentation of liver metastases on volumetric CT images. Medical Physics, 2015, 42, 6283-6293.	1.6	30
70	Hybrid detection of lung nodules on CT scan images. Medical Physics, 2015, 42, 5042-5054.	1.6	50
71	The Multimodal Brain Tumor Image Segmentation Benchmark (BRATS). IEEE Transactions on Medical Imaging, 2015, 34, 1993-2024.	5.4	3,589
72	Seizure localization using ictal phase-locked high gamma. Neurology, 2015, 84, 2320-2328.	1.5	95

#	Article	IF	CITATIONS
73	Determining the Variability of Lesion Size Measurements from CT Patient Data Sets Acquired under "No Change―Conditions. Translational Oncology, 2015, 8, 55-64.	1.7	26
74	The who and what of imaging in sarcoma and correlation with survival Journal of Clinical Oncology, 2015, 33, 10511-10511.	0.8	0
75	Variability in Assessing Treatment Response: Metastatic Colorectal Cancer as a Paradigm. Clinical Cancer Research, 2014, 20, 3560-3568.	3.2	16
76	Test–Retest Reproducibility Analysis of Lung CT Image Features. Journal of Digital Imaging, 2014, 27, 805-823.	1.6	216
77	Comparison of 1D, 2D, and 3D Nodule Sizing Methods by Radiologists for Spherical and Complex Nodules on Thoracic CT Phantom Images. Academic Radiology, 2014, 21, 30-40.	1.3	39
78	Exploring Variability in CT Characterization of Tumors: A Preliminary Phantom Study. Translational Oncology, 2014, 7, 88-93.	1.7	108
79	Monitoring Responses to Therapy in Oncology. , 2014, , 155-171.		1
80	Semi-automated validation of centralized independent review of radiological data in the OPUS trial Journal of Clinical Oncology, 2014, 32, 542-542.	0.8	0
81	Segmentation of lung lesions on CT scans using watershed, active contours, and Markov random field. Medical Physics, 2013, 40, 043502.	1.6	85
82	Exploring intra- and inter-reader variability in uni-dimensional, bi-dimensional, and volumetric measurements of solid tumors on CT scans reconstructed at different slice intervals. European Journal of Radiology, 2013, 82, 959-968.	1.2	76
83	The Imaging Viewpoint: How Imaging Affects Determination of Progression-Free Survival. Clinical Cancer Research, 2013, 19, 2621-2628.	3.2	20
84	Quantitative X-ray Computed Tomography Peritoneography in Malignant Peritoneal Mesothelioma Patients Receiving Intraperitoneal Chemotherapy. Annals of Surgical Oncology, 2013, 20, 553-559.	0.7	9
85	Abdominal Fat Is Associated With Lower Bone Formation and Inferior Bone Quality in Healthy Premenopausal Women: A Transiliac Bone Biopsy Study. Journal of Clinical Endocrinology and Metabolism, 2013, 98, 2562-2572.	1.8	165
86	Epidermal Growth Factor Receptor Mutation in Lung Adenocarcinomas: Relationship with CT Characteristics and Histologic Subtypes. Radiology, 2013, 268, 254-264.	3.6	156
87	Harnessing Technology to Improve Clinical Trials: Study of Real-Time Informatics to Collect Data, Toxicities, Image Response Assessments, and Patient-Reported Outcomes in a Phase II Clinical Trial. Journal of Clinical Oncology, 2013, 31, 2004-2009.	0.8	38
88	Multiphasic contrastâ€enhanced MRI: Singleâ€slice versus volumetric quantification of tumor enhancement for the assessment of renal clearâ€cell carcinoma fuhrman grade. Journal of Magnetic Resonance Imaging, 2013, 37, 1160-1167.	1.9	35
89	A randomized single blind controlled trial of beads versus doxorubicin-eluting beads for arterial embolization of hepatocellular carcinoma (HCC) Journal of Clinical Oncology, 2013, 31, 143-143.	0.8	7
90	Minor response rate to predict patient survival Journal of Clinical Oncology, 2013, 31, 3635-3635.	0.8	0

#	Article	IF	CITATIONS
91	Measurement of Tumor Volumes Improves RECIST-Based Response Assessments in Advanced Lung Cancer. Translational Oncology, 2012, 5, 19-25.	1.7	96
92	<i>EGFR</i> Exon 19 Insertions: A New Family of Sensitizing <i>EGFR</i> Mutations in Lung Adenocarcinoma. Clinical Cancer Research, 2012, 18, 1790-1797.	3.2	134
93	Assessing the effect of CT slice interval on unidimensional, bidimensional and volumetric measurements of solid tumours. Cancer Imaging, 2012, 12, 497-505.	1.2	24
94	Quantitative contrast peritoneography for intraperitoneal chemotherapy Journal of Clinical Oncology, 2012, 30, e13064-e13064.	0.8	0
95	Relationship of variability in tumor measurement and response assessment Journal of Clinical Oncology, 2012, 30, 2541-2541.	0.8	0
96	Real-time informatics to collect data, toxicities, image response assessments, and patient-reported outcomes (PROs) in a phase II clinical trial Journal of Clinical Oncology, 2012, 30, e19647-e19647.	0.8	0
97	Variability of Lung Tumor Measurements on Repeat Computed Tomography Scans Taken Within 15 Minutes. Journal of Clinical Oncology, 2011, 29, 3114-3119.	0.8	136
98	The Lung Image Database Consortium (LIDC) and Image Database Resource Initiative (IDRI): A Completed Reference Database of Lung Nodules on CT Scans. Medical Physics, 2011, 38, 915-931.	1.6	1,659
99	Evaluation of 1D, 2D and 3D nodule size estimation by radiologists for spherical and non-spherical nodules through CT thoracic phantom imaging. , 2011, , .		4
100	A Pilot Study of Volume Measurement as a Method of Tumor Response Evaluation to Aid Biomarker Development. Clinical Cancer Research, 2010, 16, 4647-4653.	3.2	104
101	Assessment of Therapy Responses and Prediction of Survival in Malignant Pleural Mesothelioma Through Computer-Aided Volumetric Measurement on Computed Tomography Scans. Journal of Thoracic Oncology, 2010, 5, 879-884.	0.5	81
102	The Use of Volumetric CT as an Imaging Biomarker in Lung Cancer. Academic Radiology, 2010, 17, 100-106.	1.3	43
103	Imaging Surrogates of Tumor Response to Therapy: Anatomic and Functional Biomarkers. Journal of Nuclear Medicine, 2009, 50, 239-249.	2.8	73
104	Evaluating Variability in Tumor Measurements from Same-day Repeat CT Scans of Patients with Non–Small Cell Lung Cancer. Radiology, 2009, 252, 263-272.	3.6	284
105	Quantitative Imaging to Assess Tumor Response to Therapy: Common Themes of Measurement, Truth Data, and Error Sources. Translational Oncology, 2009, 2, 198-210.	1.7	49
106	Computed Tomography Assessment of Response to Therapy: Tumor Volume Change Measurement, Truth Data, and Error. Translational Oncology, 2009, 2, 216-222.	1.7	35
107	Malignant lesion segmentation in contrastâ€enhanced breast MR images based on the markerâ€controlled watershed. Medical Physics, 2009, 36, 4359-4369.	1.6	44
108	CT-guided automated detection of lung tumors on PET images. Proceedings of SPIE, 2008, , .	0.8	8

#	Article	IF	CITATIONS
109	Prospective Assessment of Discontinuation and Reinitiation of Erlotinib or Gefitinib in Patients with Acquired Resistance to Erlotinib or Gefitinib Followed by the Addition of Everolimus. Clinical Cancer Research, 2007, 13, 5150-5155.	3.2	279
110	Marker-controlled watershed for lymphoma segmentation in sequential CT images. Medical Physics, 2006, 33, 2452-2460.	1.6	66
111	Automated Quantification of Body Fat Distribution on Volumetric Computed Tomography. Journal of Computer Assisted Tomography, 2006, 30, 777-783.	0.5	68
112	Shape-Constraint Region Growing for Delineation of Hepatic Metastases on Contrast-Enhanced Computed Tomograph Scans. Investigative Radiology, 2006, 41, 753-762.	3.5	34
113	Lung Cancer: Computerized Quantification of Tumor Response—Initial Results. Radiology, 2006, 241, 892-898.	3.6	109
114	Automated matching and segmentation of lymphoma on serial CT examinations. Medical Physics, 2006, 34, 55-62.	1.6	10
115	Pulmonary Metastases: Effect of CT Section Thickness on Measurement—Initial Experience. Radiology, 2005, 234, 934-939.	3.6	52
116	Liver segmentation for CT images using GVF snake. Medical Physics, 2005, 32, 3699-3706.	1.6	113
117	Lymph node segmentation from CT images using fast marching method. Computerized Medical Imaging and Graphics, 2004, 28, 33-38.	3.5	52
118	Automatic liver contour segmentation using GVF snake. , 2004, 5370, 1466.		4
118 119	Automatic liver contour segmentation using GVF snake. , 2004, 5370, 1466. Characterization of Small Nodules by Automatic Segmentation of X-ray Computed Tomography Images. Journal of Computer Assisted Tomography, 2004, 28, 372-377.	0.5	4
	Characterization of Small Nodules by Automatic Segmentation of X-ray Computed Tomography Images.	0.5	
119	Characterization of Small Nodules by Automatic Segmentation of X-ray Computed Tomography Images. Journal of Computer Assisted Tomography, 2004, 28, 372-377. Automatic detection of small lung nodules on CT utilizing a local density maximum algorithm.		7
119 120	Characterization of Small Nodules by Automatic Segmentation of X-ray Computed Tomography Images. Journal of Computer Assisted Tomography, 2004, 28, 372-377. Automatic detection of small lung nodules on CT utilizing a local density maximum algorithm. Journal of Applied Clinical Medical Physics, 2003, 4, 248-260. Automatic detection of small lung nodules on CT utilizing a local density maximum algorithm.	0.8	7 98
119 120 121	Characterization of Small Nodules by Automatic Segmentation of X-ray Computed Tomography Images. Journal of Computer Assisted Tomography, 2004, 28, 372-377. Automatic detection of small lung nodules on CT utilizing a local density maximum algorithm. Journal of Applied Clinical Medical Physics, 2003, 4, 248-260. Automatic detection of small lung nodules on CT utilizing a local density maximum algorithm. Journal of Applied Clinical Medical Physics, 2003, 4, 248-260. Small Pulmonary Nodules: Volumetrically Determined Growth Rates Based on CT Evaluation.	0.8 0.8	7 98 97
119 120 121 122	Characterization of Small Nodules by Automatic Segmentation of X-ray Computed Tomography Images. Journal of Computer Assisted Tomography, 2004, 28, 372-377. Automatic detection of small lung nodules on CT utilizing a local density maximum algorithm. Journal of Applied Clinical Medical Physics, 2003, 4, 248-260. Automatic detection of small lung nodules on CT utilizing a local density maximum algorithm. Journal of Applied Clinical Medical Physics, 2003, 4, 248-260. Small Pulmonary Nodules: Volumetrically Determined Growth Rates Based on CT Evaluation. Radiology, 2000, 217, 251-256. Two-dimensional multi-criterion segmentation of pulmonary nodules on helical CT images. Medical	0.8 0.8 3.6	7 98 97 547
119 120 121 122 123	Characterization of Small Nodules by Automatic Segmentation of X-ray Computed Tomography Images. Journal of Computer Assisted Tomography, 2004, 28, 372-377. Automatic detection of small lung nodules on CT utilizing a local density maximum algorithm. Journal of Applied Clinical Medical Physics, 2003, 4, 248-260. Automatic detection of small lung nodules on CT utilizing a local density maximum algorithm. Journal of Applied Clinical Medical Physics, 2003, 4, 248-260. Small Pulmonary Nodules: Volumetrically Determined Growth Rates Based on CT Evaluation. Radiology, 2000, 217, 251-256. Two-dimensional multi-criterion segmentation of pulmonary nodules on helical CT images. Medical Physics, 1999, 26, 889-895. Small Pulmonary Nodules: Evaluation with Repeat CTâ€"Preliminary Experience. Radiology, 1999, 212,	0.8 0.8 3.6 1.6	7 98 97 547 75